TINKER

FABRICATION OF SENSOR PACKAGES ENABLED BY ADDITIVE MANUFACTURING

= Deliverable D5.4 =

Prototypes of TINKER inkjet materials

This project has received funding from the European Union's Horizon 2020 research and innovation programme under the Grant agreement n°958472, project TINKER.

DT-FOF-07-2020
Assembly of micro parts (RIA)

TINKER

FABRICATION OF SENSOR PACKAGES ENABLED BY ADDITIVE MANUFACTURING

Starting date of the project: 01/10/2020
Duration: 36 months

= Deliverable D5.4 =

Prototypes of TINKER inkjet materials

Due date of deliverable: 31/12/2021
Actual submission date: 26/01/2022

Responsible WP: Michael Haslinger, WP5, PROFACTOR GmbH
Responsible TL: Ayala Kabla, PV NANOCELL LTD
Revision: V1.2

AUTHOR

Author	Institution	Contact (e-mail, phone)
Ayala Kabla	PVN	ayala@pvnanocell.com
Dieter Holzinger	TIG	dieter.holzinger@tiger-coatings.com

DOCUMENT CONTROL

Document version	Date	Change
V1.0	08.11.2021	Draft template prepared
V1.1	15.12.2021	Reviewed version
V1.2	24.01.2022	Finalized version, released by coordinator

VALIDATION

Reviewers		Validation date
Task Leader	Ayala Kabla	29.11.2021
Work Package Leader	Michael Haslinger	20.01.2022
Coordinator	Leo Schranzhofer	24.01.2022

DOCUMENT DATA

Keywords	
Point of Contact	Name: Ayala Kabla Partner: PV Nano Cell Ltd Address: 8 Hamasger st., P.O. Box 236, Migdal Ha'Emek, 2310102 Israel Phone: E-mail: ayala@pvnanocell.com
Delivery date	25.01.2022

Executive Summary

Within the framework of this project, new inkjettable materials get developed. PV Nano Cell Ltd. (PVN) is developing high metal content copper UV curable inks which will enable conductive patterns with appropriate physical structure compatible with rigid and flexible polymeric substrates. TIGER Coatings GmbH (TIG, Tiger) is developing UV-(LED) curable dielectric materials with low shrinkage properties and inks with high thermal conductivity to allow a sufficient heat transport through the material. In the course of the developments, materials have been tested and characterized by the consortium especially by Bosch (BOS), PROFACTOR (PRO), and the Foundation for Research and Technology-Hellas (FORTH).

In this report, prototypes of Electrically conductive silver and copper inks by PVN, Dielectric inks based on BMI material by PVN and based on acrylic –material by TIG and thermal conductive ink by TIG. These developments are based on results already reported in previous deliverables.

Table of Contents

1. Introduction

The vision of TINKER is to provide a new cost- and resource efficient pathway for RADAR and LIDAR sensor package fabrication with high throughput up to 250units/min, improved automation by 20%, improved accuracy by 50% and reliability by a factor of 100 to the European automotive and microelectronic industry via additive manufacturing and inline feedback control mechanisms. Autonomous driving and self-driving cars represent one prominent example for the use of microelectronics and sensor, most importantly RADAR and LIDAR sensors. Their respective markets have a big potential, e.g. it is estimated that the market size of LIDAR in automotive will double itself in the next two years (within 2020 to 2022).

Figure 1: TINKER overview

The public awareness and the industrial need for further miniaturization of such sensor packages is the main driver of ongoing efforts in the automotive sector to be able to integrate such devices into the car body like in the bumpers and head lamps instead of attaching them (e.g. on top of the car in case of LIDAR device). Safety (for the driver and others) is the most important key aspect of the automotive sector. Therefore, high-value and high-performance RADAR and LIDAR systems are required for advanced driver-assistance systems (ADAS) as well as robotic cars. Current bottlenecks are the relatively large size of such sensor devices, their weight and power consumption. Since these factors are highly limited within cars, further miniaturization and improving functionality and efficient use of resources is highly demanded.

1.1. Description of deliverable

Prototypes of Electrically conductive silver and copper inks by PVN, Dielectric inks based on BMI material by PVN and based on acrylic –material by TIG and thermal conductive ink by TIG. Based on the definitions in D2.1 and D2.5.

2. Results and Discussion

2.1. Acrylic based dielectric ink development

During the first 12 months of the project, Tiger provided first versions of the standard dielectric material and the heat conductive insulating inks. In a first instance, the evolution steps of the standard dielectric material will be discussed.

The standard material is based on a high content of epoxy-polymeric chains that are functionalized with acrylic groups. The cured material shows high thermo-mechanical properties as shown in the following table.

Table 1: Overview of mechanical properties of the dielectric material

Name	**Elastic**	**Max Force**	**Max Stress**	**Break Force**	**Break Stress**	**Break Stroke Strain**	**LASE1 Stress**
	Stroke Strain 0.025-0.3%	**Calc. at Entire Areas**	**Calc. at Entire Areas**	**Sensitivity: 10**	**Sensitivity: 10**	**Sensitivity: 10**	**Stroke Strain 1%**
Units	GPa	kN	N/mm^2	kN	N/mm^2	%	N/mm^2
Average Non Cured	2.81812	1.16676	28.709	1.16676	28.709	1.08161	23.3578
Average UV post cure	2.4107	1.16227	29.5803	1.16227	29.5803	1.41164	23.3139
Average Oven cured	2.59733	1.47038	36.6834	1.47038	36.6834	1.59551	25.4047

As can be seen in Table 1 the properties heavily depend on the curing state of the tested samples. A total curing of the specimens is essential to achieve the full mechanical performance of the printed parts. In this case post curing using an oven proved to be the most effective way to achieve a full degree of post curing.

In Figure 2, the breakthrough voltage of the printed specimens is shown.

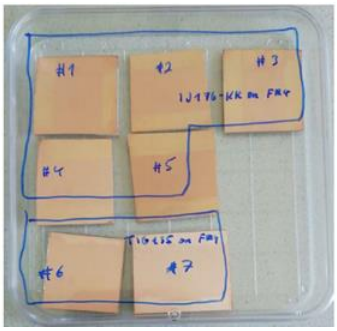

Ink	**Thickness (µm)**	**Breakthrough Voltage (kV)**	**V/µm**
IJ176-kk	17.1	2.9	170
IJ176-kk	19.6	4.0	204
IJ176-kk	24.1	2.0 (Layer was damaged during test)	-
IJ176-kk	6.0	1.0	167

Figure 2: Printed parts and the resulting breakthrough voltage

The average breakthrough voltage was in the range of 180 V/µm, fulfilling the required 40V/µm easily.

This version is now also available in translucent white and translucent black allowing structured printing in different shades. The mechanical properties are comparable as shown in Figure 3. The different bars correspond to the respective printing direction. Depending on the printing angle, slight differences were observed.

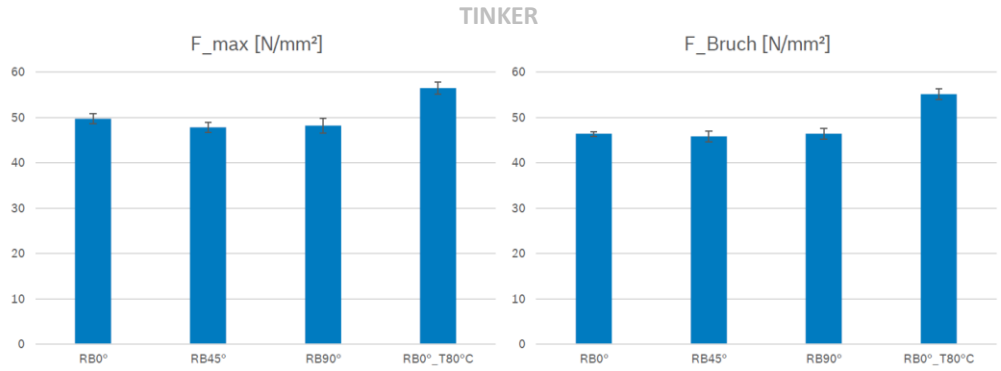

Figure 3: Mechanical properties of the translucent black 3D printing inks.

In a second stage, inks based on dendrimeric structures were formulated. In Figure 4, a dendrimeric structure is shown.

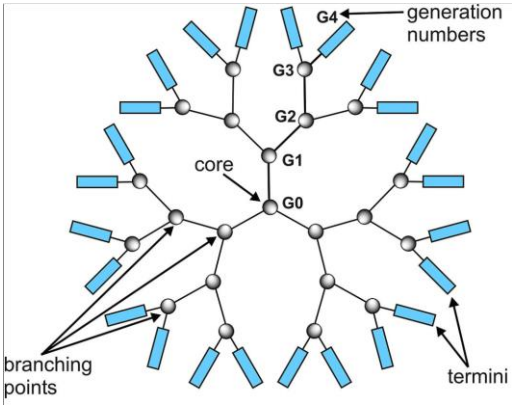

Figure 4: Model of a dendrimeric structure

These sterically highly demanding structures with acrylate functionalities at the end of each branch allow the realization of a high crosslinking density on the one hand and on the other hand show a reduced shrinkage during the curing process. Additionally, these molecules show significantly reduced viscosities which is also advantageous for the inkjet printing process. So far, several different structures were evaluated resulting in inks which show significantly reduced viscosity and shrinkage but still offer reasonable mechanical strength.

Table 2: Overview of the mechanical strength of the dendrimeric inks

Name	Elastic	Max Force	Max Stress	Break Force	Break Stress	Break Stroke Strain	LASE1 Stress	Elongation /Area
Parameter	**Stroke Strain 0.025-0.3% [GPa]**	**Calc. at Entire Areas [kN]**	**Calc. at Entire Areas [N/mm²]**	**Sensitivity: 10 [kN]**	**Sensitivity: 10 [N/mm²]**	**Sensitivity: 10 [%]**	**Stroke Strain 1% [N/mm²]**	**[%/mm²]**
Total Range	0.14109	0.83087	20.7718	0.83087	20.7718	4.45994	0.35476	11.1498
Total Standard	0.04747	0.34453	8.61325	0.34453	8.61325	1.74391	0.13005	4.35976

Compared to the first inks showing a viscosity of 20 – 25 mPas at 50 °C, the dendrimeric inks have viscosity values of 8 – 10 mPas at 50 °C. These low viscosity values allowed the incorporation of inorganic, heat conductive nanoparticles.

Boron nitride and Silicon carbide were chosen as heat conductive materials as both materials are available as nanoparticles. In first pre-trial evaluations, compatible dispersing agents which can wet the surface of these materials and stabilize them to a certain degree in the inks, were identified. The developed formulations were then

grinded on a bead mill equipped with ceramic beads to avoid the contamination of the inks with metal particles. The aim of the bead mill treatment was not grinding the primary particles, but improving the dispersion of agglomerates in the mixture. Due to the small size of the particles a huge amount of "fresh surface" was generated during the grinding process leading to an increase of viscosity in the course of the grinding. To a certain degree, the effect was reduced by adding additional dispersing agent; therefore it was of high importance having an ink matrix with a rather low viscosity to make sure that a significant amount of the heat conductive nanoparticles was integrated in the ink maintaining a reasonable viscosity to allow jetting in a standard inkjet print-head. In Table 3, the stability of viscosity over time for the different inks is shown. Whereas the SiC filled inks didn´t exhibit stable viscosity over a one month period, the BN filled ink was very stable showing basically no change in viscosity.

Table 3: Viscosity over time for the heat conductive inks

Ink number	Filler	Start viscosity [mPas]	+ 7 days [mPas]	+ 14 days [mPas]	+ 21 days [mPas]	+ 28 days [mPas]
IJ980A-A	SiC	19,7	22,3	24,6	26,8	28,4
IJ982A-A	BN	19,9	19,8	19,3	19,4	18,7

The inks were filtered with a 5 µm filter to remove all particles which were too big for jetting. The respective BN filled ink was sent to Profactor to perform first printing trials. Due to the high particle loading, Profactor had difficulties jetting the inks with the available disposable Spectra Dimatix head. The only way at that time to obtain samples for heat conductivity measurements was by using molds to obtain some casted cured samples with defined dimensions. Molds were fabricated for the generation of samples by brushing ink into the mold for first thermal conductivity measurements, due to a very long printing time of samples with the required volume. In Figure 5 and Figure 6, the obtained samples are shown.

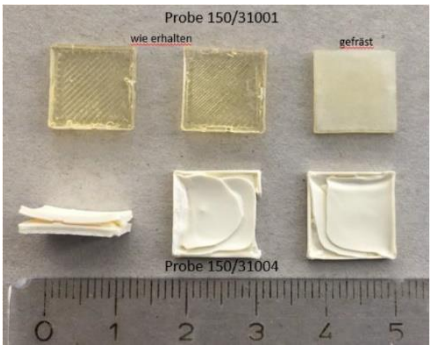

Figure 5: Casted samples of 150/31001 (standard dielectric ink) and 150/31004 (BN-filled ink)

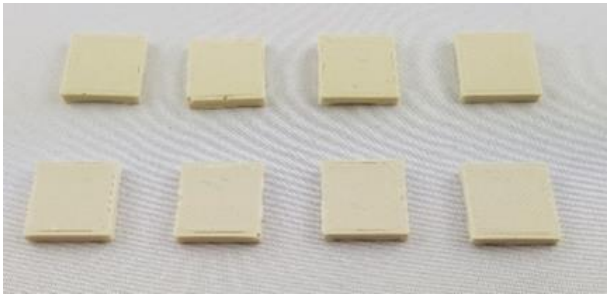

Figure 6: Samples for thermal conductivity measurements at Bosch, fabricated by brushing into a mold and repetitive UV-curing at Profactor.

While the standard dielectric inks could be cured in the mold without any issues, the BN filled ink was difficult to cure due to the high inorganic content. A trial was conducted to fill the respective mold layer by layer with an intermediate curing step. Nevertheless, the casted specimens broke apart during shipment due to the presence of uncured material. In Table 4, the results of the first heat conductivity measurements performed by Bosch are summarized.

Table 4: comparison of the heat conductivity of the standard dielectric inks and the BN-containing inks

Probe	**01) 150/31001 (Standard Dielectric ink)**	**02) 150/31004 (BN-filled ink)**
Temperature	**Heat Conductivity (W/mK)**	**Heat Conductivity (W/mK)**
25°C	0.21	0.29
50°C	0.22	0.29
75°C	0.23	0.29
100°C	0.23	0.29
125°C	0.24	0.30
150°C	0.24	0.30

Based on the measured values, an increase of the heat conductivity by 25 % to 40 % was measured with the addition of BN particles. It should be mentioned however, that the heat conductivity measurements were inconclusive due to the test specimens not being entirely suitable for the measurements.

In order to allow more significant measurements, Profactor fabricated samples by inkjet printing as well, showing good compatibility of the ink with industrial KM512-printheads, as proper jetting behavior could be sustained over the whole printing procedure without considerable nozzle failures. First samples delaminated from the substrate surface, which could be prevented by a proper pretreatment of the used PET-foil. The achieved thermal conductivities were in good accordance with each other and the brushing process was thus approved for quick characterizations of new ink formulations that are not ready for the printing process yet.

Since ink IJ982A-A tends to build agglomeration after longer storage times, which potentially lowers the achievable thermal conductivity as a lower share of heat transferable medium is available, another set of samples was fabricated after a proper shaking procedure that eliminated all agglomerations , and sent to Bosch for additional thermal conductivity measurements. Furthermore, new ink formulations, including an ink with higher share of boron-nitrite nanoparticles and inks with silicon-carbonate, were provided by Tiger and will be used for sample fabrication in the next iteration. Some of the samples also contain a certain amount of solvent to further increase the solid loading of the printed samples in the dried/cured state. It is expected that the new inks will exhibit an increase in heat conductivity.

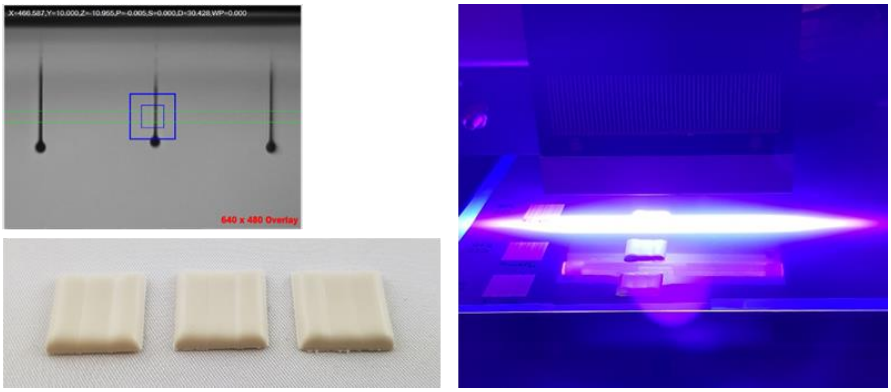

Figure 7: Drop formation during jetting and resulting inkjet printed samples for thermal conductivity measurements. At first, delamination occurred during UV-curing but could be prevented by adaption of the base substrate.

The 3D-structure of a waveguide antenna was designed by Bosch and first printing trials for characterization of the antenna wall printability were performed at Profactor. In order to allow a metallization of the antenna by inkjet printing, the printing experiment included structures with walls not perpendicular to each other, but at angles slightly smaller than 90° in relation to the surface. However, the dielectric ink did not allow the intended angles, as the wetting behavior of the material on itself is not optimal for small area – patterns and high thicknesses of several millimeters.

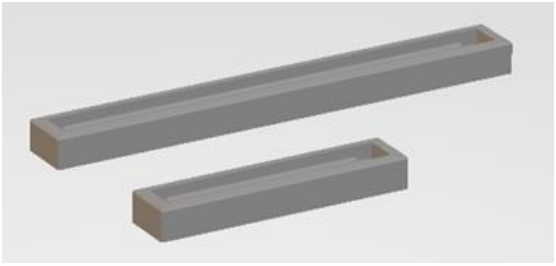

Figure 8: 3D-Design of a waveguide antenna test structure

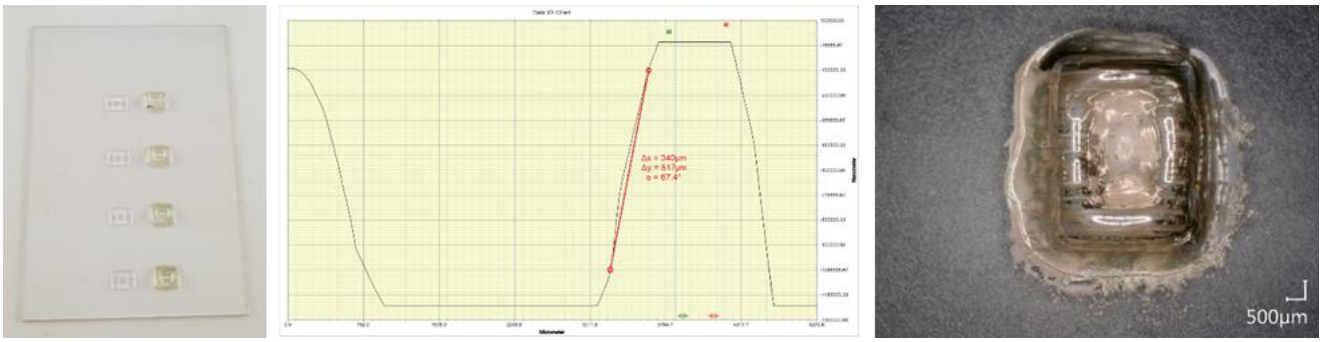

Figure 9: Inkjet printed test structures imitating the antenna walls, resulting profile with lower angle than intended and microscope picture after inkjet metallization.

Future investigations will include printing trials with different dielectric inks. Since the development of a fabrication process for 3D-structures is quite time consuming, a script for the automation of the whole printing process including the required functionalities (different printing patterns for each layer, changing substrate height, etc.), was developed for the inkjet printer at Profactor to allow more and faster printing experiments that will include different geometries and adapted fabrication strategies in future.

2.2. Solvent based metal inks

Nano Ag and Cu solvent-based inks listed in Table 5 were provided by PV Nano Cell to Profactor, for printing and sintering testing.

Table 5: Solvent based ink prototypes

Ink	Batch	%Metal	Particle size (µm)	Surface tension (dyn/cm)	Viscosity @25°C (cP)	Resistivity (µΩcm)
I50TM-119	W276	50% Ag	D50~70nm, d90~120nm	29	38	10.1 (130°C/30min)
IC50TM-8	KP123	50% Cu	D50=50nm, d90=118nm	32	30	≤35 (laser sintering)

The particle morphology of the silver and copper inks are exhibited in Figure 10, where the average particle size of silver is around 70 nm, and the average size of copper is around 50 nm.

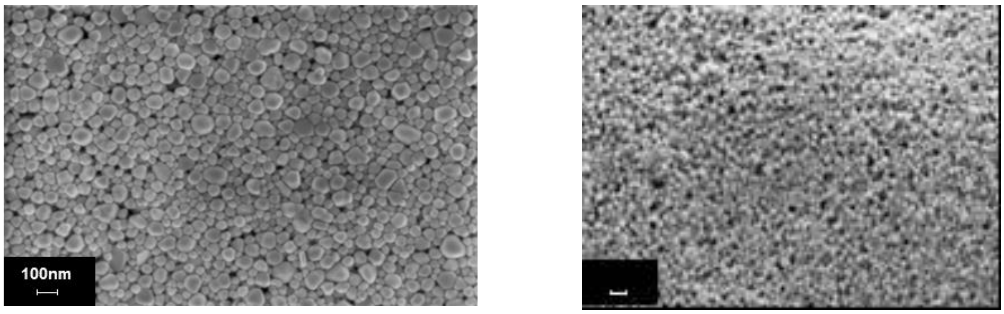

Sicrys™ Ag NP ink, D50 ~70nm, D90 ~120nm

Sicrys™ Cu NP ink, D50 ~50nm, D90 ~120nm

Figure 10: High resolution scanning electron microscope images of Ag particles (left) and Cu particles (right).

Solvent-based silver ink I50TM-119 was printed with a KM1024i-MHE print head on PET-CT7 and FR4 substrates, while the solvent-based copper ink IC40DM-7 was printed with a DMC-11610 (10pL) cartridge on Kapton as shown in Figure 11. Reference thermal sintering at PV Nano Cell showed 11-14 times bulk for Ag/PET samples, 7-15 times bulk for Ag/FR4 samples. The thickness of the samples varied between 2 to 7.5 µm for the Ag/PET samples and 1 to 6 µm for the Ag/FR4 samples. The copper ink could not be sintered thermally as a reference due to its high sintering temperature of 270°C.

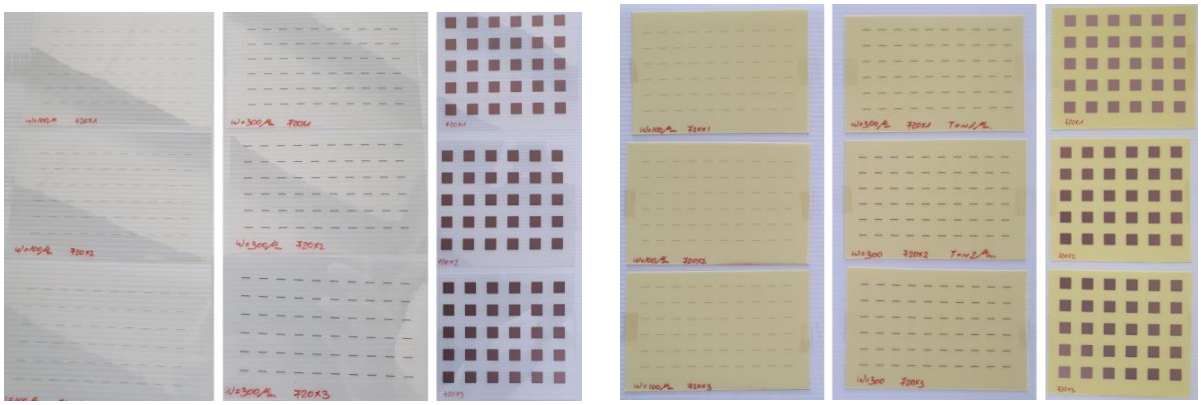

Figure 11: Inkjet-printed silver on PET substrate (left). Inkjet-printed silver on FR4 substrate (right). 1, 2, and 3 layer thickness. 100 µm and 300 µm width, 5 mm length lines. 10 mm x 10 mm squares.

For NIR (Near infrared) sintering of solvent based silver ink, an emitter by Adphos, type UB-54-250 (5.4kW), MPP120 radiation module was used. Up to 6 emitters were situated transversal to the transport direction. Results show <3 x bulk resistivity of Sicrys™ Ag was achievable on PET, PEN and glass substrates. Sintered lines were of ~500-700µm width and 2.5-13 µm thickness. The energy required for sintering on PEN and PET is lower than glass, due to the difference in thermal conductivity of the substrates

a. Thermal conductivities @RT: ~0.15 W/mk PEN, ~0.15-0.4 W/mk PET, ~0.94 W/mk glass
b. Fluence for<3xbulk resistivity: 11-13 J/cm^2 on PEN, ~20 J/cm^2 on PET, 1080 J/cm^2 on glass

Laser sintering feasibility was performed at PV Nano Cell on lines printed with the copper ink on FR4 substrate. The laser was a 532nm, DPSS, continuous wave, gaussian beam profile. Resistance measurements were carried out with a 4-point-probe, PicoTest M3511A, thickness was measured with a Dektak IIA profilometer, and width was measured with a digital microscope. Four layers printed exhibited a line thickness of ~4-6.5 µm and resistivity of 3.4-4.4 xbulk. Adhesion test showed a light trace of the line on the tape, with most of the line remaining on the FR4 substrate. (Table 6)

Table 6: Laser sintered Cu/FR4 parameters and measurements

Line	Beam Ht. (mm)	Motion speed (mm/s)	Voltage (V)	Power (W)	Resistance (Ω)	Width (µm)	Avg. H (µm)	Resistivity (µΩcm)	Resistivity (xBulk)
5F-A1	0	5	3.6	0.7	0.237	123	6.5	7.5	4.4
5F-B1	0	5	3.6	0.7	0.240	161	4.6	7.1	4.2
5F-C1	0	5	3.6	0.7	0.220	154	4.3	5.8	3.4
5F-D1	0	5	3.6	0.7	0.230	157	4.2	6.1	3.6

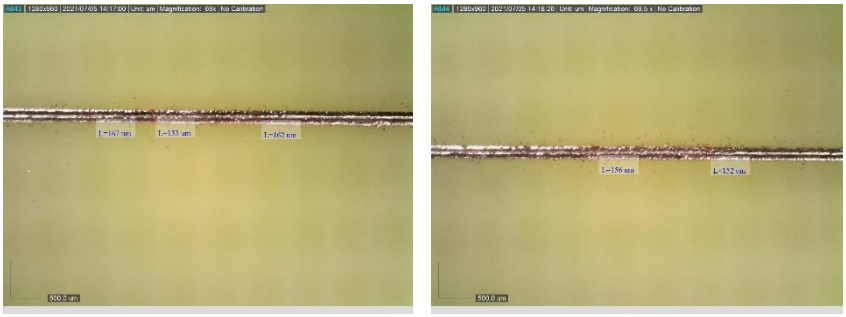

Figure 12. Digital microscope image examples of sintered lines 5F-B1 (left) and 5F-C1 (right)

The copper nanoparticle ink IC50TM-8 was successfully printed on glass substrates by Profactor, where the observed wetting was satisfying. The pattern dimensions were set to 0.5x10mm and 0.5x20mm and they were dried on a hotplate at 80°C for 10 minutes before sintering with a flash mercury lamp operating in the visible wavelength range. The applied dose was 0.5 W/cm^2 for all samples, in order to minimize the number of unknowns when establishing a relation between the material thickness and the resulting resistance.

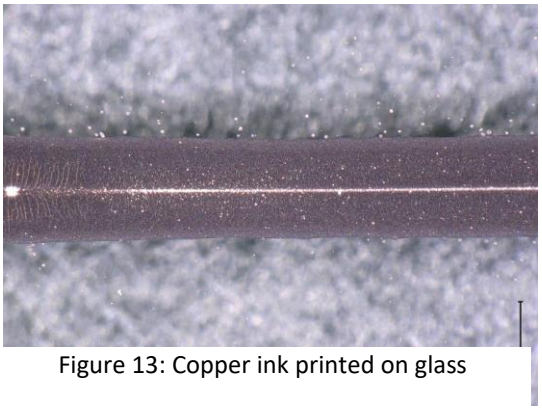

Figure 13: Copper ink printed on glass

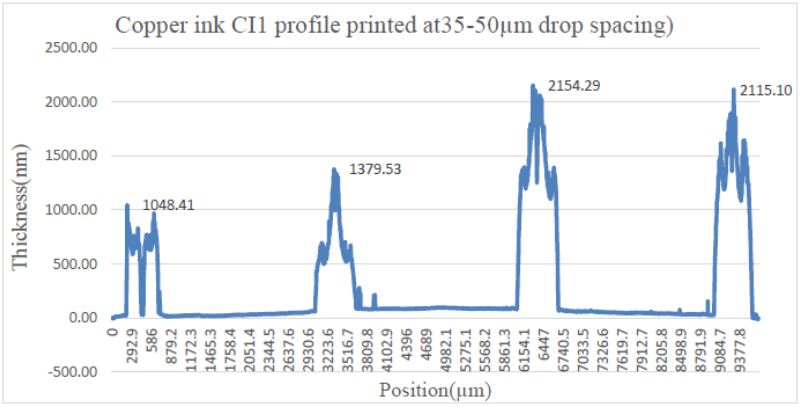

Figure 14: Profile of copper ink printed on glass in 35-50µm drop spacing resolution

The relation between the resulting material thickness and the average measured surface resistance of the samples are shown for the glass substrate (using the mentioned flash sintering method) and in Figure 16 for samples on Kapton foil, which were post-processed using laser sintering by a CW laser, 2W, 808nm. All samples were printed with identical settings, only varying the printing

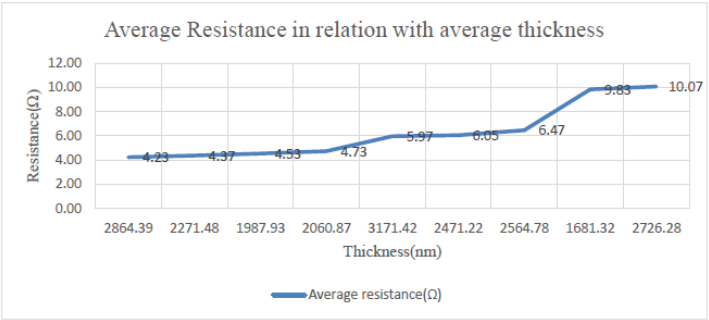

Figure 15: Average resistance in relation to average thickness of printed copper on glass.

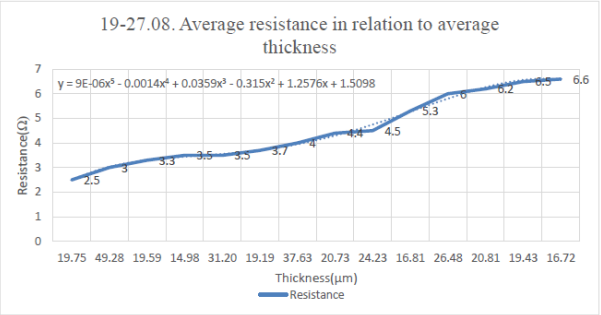

Figure 16: Average resistance in relation to maximal thickness of printed copper on Kapton foil.

resolution to manipulate material heights.

Table 7: Average resistance of printed silver.

Sample	Average Resistance (Ω)
Sample 1	0.0477
Sample 2	0.0595
Sample 3	0.0530
Sample 4	0.0502
Sample 5	0.0479
Overall Average	0.0517
Standard Deviation	0.0049

In comparison to copper ink printed on glass, the same experiment with silver nanoparticle ink I50TM-119 achieved results with distinctly less resistance, which was in the range of 0.05-0.06Ω as shown in Table 7.
Further experiments included also the printing of copper and silver nanoparticle inks on both PET and acrylate based substrates. The sample dimensions were 0.3x10mm and 0.5x10mm and the wetting behavior was satisfying. However, the results of both sintering methods proved to be unsuitable for these two types of substrates. In both cases the printed copper samples were either completely or partially destroyed, using the same parameters as for the previous substrates (Kapton and glass), and different settings did not achieve better results.

2.3. UV curable silver ink

A UV curable silver ink prototype from PV Nano Cell was provided to Profactor for testing with 55% Ag and monomer content 7% (Table 8). The particle size was d50 ~70nm and d90 of ~120nm. The viscosity of the ink was 27 cP at 25°C, suitable for a Konica Minolta head or Xaar, and resistivity of 14 µΩ·cm from 200°C/1hr sintering temperature (
Table 9).

Table 8: I55TM-464U formulation composition

Component	I55TM-464U
Ag (wt %)	55.00
Dispersant (wt %)	1.10
Monomer (wt %)	6.88
Photoinitiator (wt %)	2.00
TGME (wt %)	35.02

Table 9: I55TM-464U ink properties

Ink	Batch	%Metal	Particle size (µm)	Surface tension (dyn/cm)	Viscosity @25°C (cP)	Resistivity (µΩcm)
I55TM-464U	W195	55% Ag	D50~70nm, d90~120nm	38	27	14 (UV + 200°C/1hr)

Experiments were performed to reduce the resistivity of the UV curable silver ink formulation I55TM-464U by incorporating an additive into the ink formulation that would decrease the percolation threshold and sintering temperature. In parallel, experiments were performed to decrease the spreading of the ink on the substrate by increasing the monomer percentage in the ink. Two additives were added to 0.5% and 1% w/w, and four monomer to silver ratios were tested, as well as sintering temperatures of 200, 150 and 130 °C. The formulations and results are indicated below, showing reduced resistivity in the formulations with the additive. However, the formulations with the additive exhibited instability over time due to polymerization. Thereby, these inks do not provide the required solution, and alternative methods need to be researched to improve resistivity.

Table 10: **UV curable formulations tested**

	Formulation No.				
Component	**UV-1**	**UV-2**	**UV-3**	**UV-4**	**UV-5**
Ag (wt%)	50%	50%	50%	50%	50.0%
Dispersant (wt%)	1.0%	1.0%	1.0%	1.0%	1.0%
Monomer (wt%)	6.3%	12.5%	6.3%	12.5%	25.1%
Photoinitiator (wt%)	2.0%	2.0%	2.0%	2.0%	2.2%
Additive 1 (wt%)	0.0%	0.0%	1.0%	1.0%	1.0%
Additive 2 (wt%)	0.0%	0.0%	0.5%	0.5%	0.5%
Solvent (wt%)	40.8%	34.5%	39.3%	33.0%	20.20%
Total (wt%)	100.0%	100.0%	100.0%	100.0%	100.0%
Ag/monomer ratio	8	4	8	4	2

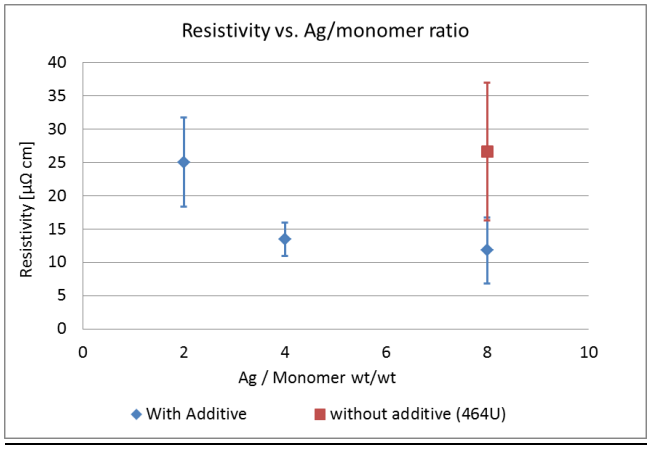

Figure 17. Ag to monomer ratio and additive influence on resistivity, and compared to formulation I55TM-464 without additive.

2.4. UV curable Cu ink

The first version of UV curable copper ink, IC45TM-61 (Table 11) was prepared by PV Nano Cell at the formulation composition similar to the UV curable Ag ink (I55TM-464U) in terms of metal to monomer ratio and monomer to photoinitiator. A stability study was performed to check suitability of the Cu particles with the monomer, testing suitability over a month and a half, showing no loss in particle stability.

Table 11: IC45TM-61 formulation composition

Component	IC45TM-61
Cu (wt %)	45.00
Dispersant (wt %)	2.25
Monomer (wt %)	5.60
Photoinitiator (wt %)	1.60
TGME (wt %)	45.55

2.5. Polyimide based dielectric ink

A candidate dielectric ink formulation based on BMI has been developed by PV Nano Cell with 50% active material in a mixture of Triethylene glycol methyl ether (TPM) and Propylene glycol monomethyl ether acetate (PMA) solvents. The measured dielectric constant was ~3 (Table 12).

Table 12. Polyimide based dielectric ink formulations

Ink	Active material	Solvent	Ink Type	Surface tension (dyn/cm)	Viscosity @25°C (cP)	Dielectric const.
DPI-50TP-1	50%	Mixture of Triethylene glycol methyl ether (TPM) and Propylene glycol monomethyl ether acetate (PMA)	Polyimide (BMI)	~29	~20	~3

2.5.1. Investigate the effect of the BMI content and the solvents PMA/TPM ratio on viscosity

Different formulations were prepared with varied BMI % and PMA: TPM ratio. The samples were tested for viscosity at 25°C. Three levels of the BMI content were tasted (50%, 25% and 12.5%) and four levels of the PMA ratio (0%,

33%, 50% and 100%) where the 0% and 100% refer to TPM and PMA as the only solvent, respectively. Table 13 presents the prepared formulations, the levels of the factors and the measured viscosity, also the calculated viscosity based on the regression model.

Table 13. Viscosity of BMI formulations

	Nominal values			
Sample #	**% TPM**	**% PMA**	**% BMI**	**Viscosity [cP] @ 25°C**
1	100%	0%	50%	46
3	100%	0%	25%	14.9
5	100%	0%	13%	9
8	67%	33%	50%	26.5
10	67%	33%	25%	7.7
12	67%	33%	12.5%	4.6
7	50%	50%	50%	20.5
9	50%	50%	25%	6
11	50%	50%	12.5%	3.5
2	0%	100%	50%	11.5
6	0%	100%	37%	5.8
4	0%	100%	25%	3.1

Samples numbered 1, 7 and 8 with 50% wt BMI were tested for viscosity at different temperatures (Table 14).

Table 14. Viscosity of select BMI formulations as influenced by temperature

	Nominal values				
Sample #	**% TPM**	**% PMA**	**% BMI**	**Temperature [°C]**	**Viscosity [cP] @ 25°C**
1	100%	0%	50%	25	46
				30	36.2
				35	28.6
				40	22.3
				45	18
8	67%	33%	50%	25	26.5
				30	21.2
				35	17.1
				40	14
				45	11.5
7	50%	50%	50%	25	20.5
				30	16.7
				35	13.7
				40	11.4
				45	9.5

Based on the results, a correlation between the viscosity and the different parameters (BMI %, PMA %, TPM % and temperature) was built. The correlation for viscosity at 25°C as a function of %PMA and % BMI is presented in the following equation:

$$Visocsity\ [cP] = 3.7006 * e^{(0.0708*(2.25-21.37*\%\,PMA+66.64*\%BMI))}$$

From the above correlation we have chosen Konica Minolta and Xaar printheads for printing tests of the formulation with 50% BMI and 50% PMA (the calculated viscosity at 25°C should be 21.5 cP). A dielectric ink prototype is being prepared for Profactor with this formulation composition. The correlation of the viscosity to %PMA, % BMI and temperature is presented in the following equation and in Figure 18.

$$Visocsity\ [cP] = 4.2367 * e^{(0.0695*(24.64-22.59*\%\,PMA+65.41*\%BMI-0.87*Temperature))}$$

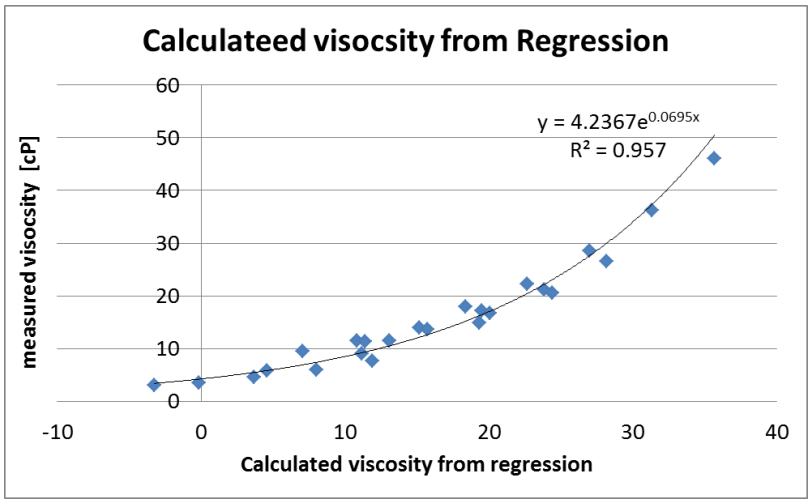

Figure 18. Measured viscosity versus calculated viscosity from regression

2.6. Inkjet materials for the RADAR use case at Bosch

In TINKER it is planned to realize two different demonstrators, the technology prototype and the RADAR function demonstrator. The focus will be the 3D inkjet printed waveguide antennas for the RADAR function demonstrators with inner metallization layer and heat dissipation for the MMIC (Monolithic Microwave Integrated Circuit).

The RADAR packages with inkjet materials (conductive material, heat dissipation material etc.) will be tested at thermal cycling -40 °C to +125 °C up to 1000 cycles and +85 °C, 85 % r.F. up to 1000 hours. These reliability tests simulate real temperature fluctuations and the humidity impact over the life cycle of an application in a shorter time. Furthermore, it is important that the inkjet materials be adjusted according to the CTE (Coefficient of Thermal Expansion) values of the PCB (Printed Circuit Board) to avoid a mismatch between printed materials and the PCB and high frequency material.

2.6.1. Thermal simulation for the heat dissipation materials

The target of the thermal simulation was the determination of the minimum volume for a heat dissipation for a 3D-printed waveguide antenna package to achieve the benchmark (allowable heating during operation approx. 86°C). The boundary conditions for the thermal simulation are:

- Power dissipation of the MMIC, 2 W
- Printed substrate material, thermal conductivity approx. 0,6 W/mK
- Estimated dimensions for the volume 45.00 x 11.00 x 0.70 mm³ over the MMIC
    - Cu-foil / plate, thermal conductivity approx. 240 W/mK
    - Printed thermally conductive material, thermal conductivity approx. 2.5 W/mK
    - Printed Ag ink, thermal conductivity approx. 120 W/mK

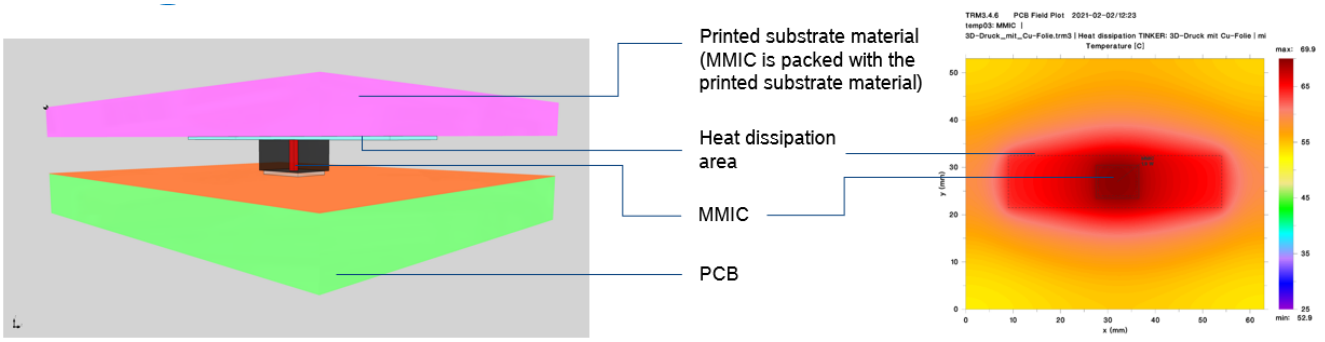

Figure 19: Construction for thermal simulation with PCB, MMIC and the heat dissipation area for the thermal conductive ink-material.

The results show that a thermal conductive material (approx. 2.5 W/mK) as printed substrate material (MMIC is packed with the printed substrate material) is not sufficient to dissipate the heat, as the left diagram in Figure 20 shows. Based on the results in the diagrams below of the thermal simulation, a Cu foil with the thickness of 300 µm and with a head dissipation area of 325 mm² is sufficient to dissipate the heat from the MMIC. Further simulation for the heat dissipation of the MMIC using inkjet printed materials can be performed again after the availability of the material properties in terms of thermal conductivity are available.

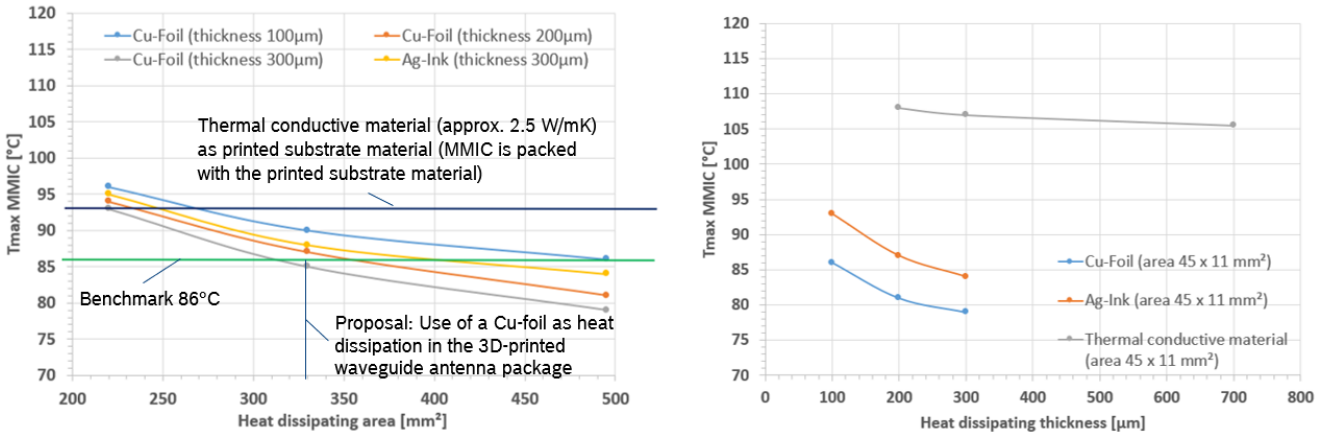

Figure 20: Results of the thermal simulations

In addition, first measurements for the determination of the thermal conductivity of Tiger dielectric inks were carried out at Bosch. In addition, first measurements for the determination of the thermal conductivity were carried out at BOS. The results of the thermal conductivity measurements show no significant differences in the thermal conductivity between the material 150/31001 and 150/31004 (150/31004 filled with Bornitride for increasing the thermal conductivity of the material) from Tiger (table **T1**). New samples for thermal conductivity measurements are currently in production by PRO.

2.6.2. Thermomechanical analysis of the inkjet materials

A thermomechanical analysis was performed with the Dielectric ink TIGITAL® UV-LED 3D ink – Series 150/3 and thermal conductive material – 150/31004 from the project partner TIG, to identify the CTE properties of the inkjet materials (Figure 21 and Figure 22). The information about the CTE properties of the inkjet materials will be important to evaluate the reliability of the RADAR package between the PCB and the inkjet materials in the temperature cycle test (-40°C to +125°C) and temperature humidity test (+85°C, 85% r.h.).

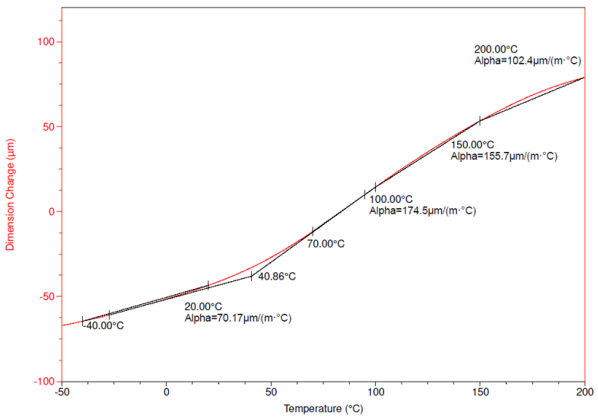

Figure 21: Thermomechanical analysis of the Dielectric ink TIGITAL® UV-LED 3D ink – Seri2es 150/3

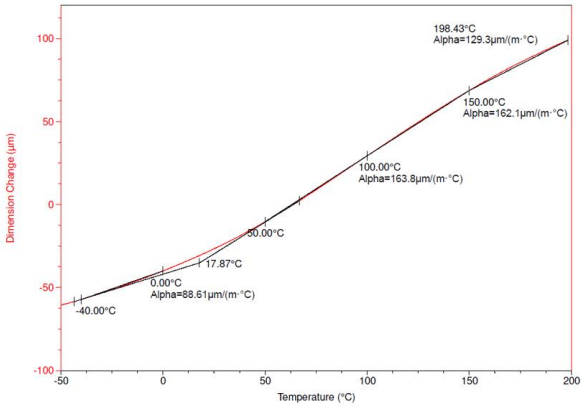

Figure 22: Thermomechanical analysis of the thermal conductive material – 150/31004

2.6.3. Inner metallized layer for the waveguide channels

A defect free inner metallized layer of the waveguides channels is required. For this purpose, Bosch has designed angle dependent waveguide channels (Figure 23) with angle variation 90°, 88°, 87° and 85° structures for inkjet-based metallization investigations at Profactor.

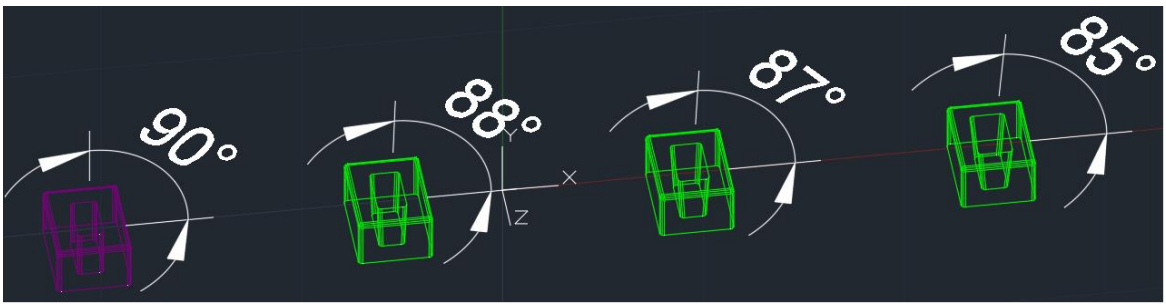

Figure 23**:** Waveguide angle variation 90°, 88°, 87° and 85° structures for inkjet-based metallization investigations

A simulative characterization of 90° angle waveguide channels has already been performed at Bosch. The main message of the simulation results is that no significant fluctuation of guided wavelength within the frequency band of interest was detected. Specifically, this means that the simulation of the proposed 3D waveguide structures (90°) appears promising in terms of line attenuation < 0.26 dB/cm (Rogers 3003, high frequency ceramic-filled PTFE laminate exhibit 0.7 dB/cm). For the simulative characterization of the waveguide properties, the material properties of the conductive ink Sicrys™I50TM-119 were assumed for a defect-free inner metallization of the waveguide structures.

3. Conclusions

Within the scope of task T5.3, Tiger has developed two iterations of acrylic based dielectric ink, the first without additive, and the second with nano Boron nitride and Silicon carbide additives to enhance the thermal conductivity. The first iteration of inks shows upon curing, high thermo-mechanical properties. The average breakthrough voltage was in the range of 180 V/µm, fulfilling the required 40V/µm. An increase in heat conductivity from 25 % to 40 % was achieved with the addition of Boron nitride additive.

As the measurement and the thermal simulation results for thermal conductive materials show, further adjustments are required to increase the thermal conductivity of the inks for the heat dissipation of the MMIC in the RADAR package. In coordination with Profactor and Tiger, further measurements on thermal conductive ink materials are in preparation.

PV Nano Cell has developed and provided conductive ink prototypes for testing to Profactor, including a solvent based silver, solvent based copper, UV curable silver, and UV curable copper. In addition, a polyimide dielectric ink was developed to suit the viscosity requirements of the Konica Minolta and XAAR heads. The metal inks have been characterized by Profactor. A dielectric ink prototype is being prepared for Profactor. Sintering by various techniques was performed, including thermal, NIR, and laser on various types of substrates: Kapton, glass, FR4, PEN, PET, acrylate. Resistivity results as low as ~3xbulk for silver on PET, PET, and glass (NIR sintering) and ~4xbulk for copper on FR4 (laser sintering) are achievable, but not on all substrates and from all sintering methods. On PET and acrylate substrates, laser sintering destroyed the copper printed lines due to the sensitivity of the substrates.

4. Outlook

After the evaluation of the results of the inkjet-based inner metallization layers of the waveguide channels fabricated at Profactor, further simulative characterization of waveguide properties regarding the waveguide angle variation 88° / 87° / 85° structures may be necessary.

A key quality feature for the RADAR package is the adhesive strength of the inkjet printed material on the copper surface and on the RF material surface of the PCB. In coordination with TINKER project partners (Profactor, Tiger and Bosch) adhesive strength tests will be carried out. It will be important to investigate the adhesion strength before and after the temperature cycle test (-40°C to +125°C) and temperature humidity test (+85°C, 85% r.h.) on the copper surface and on the RF surface of the PCB.

5. Degree of Progress

The corresponding task T5.3 activities have been fulfilled. The electrically conductive, dielectric, and thermally conductive material prototypes have been developed and characterized in terms of functional property.